

# Optimizing Hydrogen and Ammonia Injection Timing for Enhanced Mixture Formation in Internal Combustion Engines

## ABSTRACT

Hydrogen and ammonia are two carbon-free alternative fuels for engines. They represent some of the most viable pathways toward achieving our objectives of energy conservation and reducing emissions. To research the quality of the hydrogen-ammonia-air mixture formation under different hydrogen/ammonia injection timing, a three-dimensional simulation model for a PFI(Port Fuel Injection)hydrogen internal combustion engine with the inlet, outlet, valves and cylinder was established using Converge software. Research focused on the space distribution characteristics and variation law of velocity field, concentration field and turbulent kinetic energy under different injection timings in order to reveal the influence of these parameters on hydrogen-ammonia-air mixture formation process. The results showed that hydrogen injection should be neither too early nor too late. Backfiring can be initiated too early or too late. Therefore, the optimum starting point for hydrogen/ammonia injection should be 338°CA.

*Keywords: Hydrogen; ammonia; Mixture distribution, injection timing.*

## 1. INTRODUCTION

In recent years, the problem of global warming caused by carbon dioxide emissions from the burning of fossil fuels has attracted considerable attention from all sectors of society, and global carbon dioxide emissions have been increasing year on year, with the burning and use of fossil fuels still accounting for a large proportion of total carbon emissions. Increasingly stringent emission regulations and the national policy direction of green and clean energy consumption have advanced the new trend of green and renewable new energy development, making the development of clean energy occupy an important position in the automotive field[1]. And hydrogen/ammonia has outstanding advantages among many alternative fuels due to its unique physical and chemical properties[2,3].

Hydrogen stands out as the most promising fuel due to its array of favorable characteristics, including its high heating value, rapid flame propagation rate, and notable reaction activity[4,5]. Benbellilconducted experiments on a dual-fuel compression-ignition engine, finding that blending natural gas with hydrogen improved combustion, reduced HC and CO emissions, but cautioned against H<sub>2</sub> concentrations exceeding 50% at high loads due to engine knock[6]. Gu evaluated the combustion and emission performance of the ammonia hydrogen mixed fuel engine. With the hydrogen mixing ratio increasing, the flame propagation speed increasing, the peak of heat release rate increasing, and the ignition timing advance[7]. Frigo investigated the performance impact of burning ammonia/hydrogen dual fuel on a four-stroke gasoline engine, noting that the load primarily influences the ammonia-to-hydrogen ratio, with ignition and combustion rates improving after adding hydrogen, albeit with slightly reduced performance compared to gasoline combustion[8].

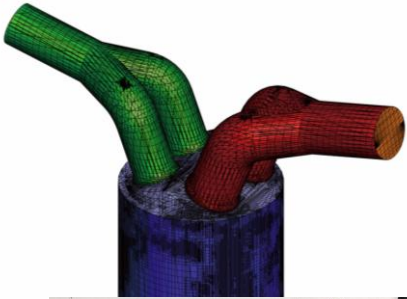
39 Wang studied the performance effects of a diesel-fueled ammonia-hydrogen hybrid engine  
40 on a high-pressure common rail compression ignition engine, revealing substantial  
41 improvements in power and economy with the addition of hydrogen fuel, while noting  
42 increased NO<sub>x</sub> emissions but significant reduction in N<sub>2</sub>O emissions beneficial for global  
43 warming mitigation[9].  
44 Pure ammonia combustion in engines poses challenges due to high boundary conditions for  
45 combustion and prolonged initial flame development[10]. Dimitriou research discovered that  
46 achieving pure ammonia combustion is challenging due to its higher ignition temperature  
47 compared to diesel, necessitating initial diesel ignition in diesel engines; however, slow  
48 flame propagation and high vaporization latent heat values hinder complete combustion,  
49 leading to ammonia escape in cases of excessive ammonia blending[11]. Common solutions  
50 involve blending combustion with carbon-containing fuels (natural gas, methanol, diesel,  
51 gasoline) and hydrogen to lower combustion boundary conditions[12,13]. Sechul  
52 investigated a natural gas/ammonia dual-fuel ignition engine, replacing over 50% of natural  
53 gas with ammonia fuel, resulting in a more than 28% decrease in CO<sub>2</sub> emissions, alongside  
54 a reduction in laminar flame propagation speed as ammonia fuel proportion increased[14].  
55 Grannell explored the combustion characteristics of ammonia/gasoline under stoichiometric  
56 conditions, and they found that there were no fixed blending ratios between ammonia and  
57 gasoline suitable for all operating conditions[15]. Sahin et al. studied the impact of co-  
58 combustions an ammonia solution (25% ammonia + 75% water) with diesel fuel on a small  
59 diesel engine, finding that while adding ammonia solution to the intake manifold enhanced  
60 engine efficiency, it worsened emissions, increasing CO, HC, and NO<sub>x</sub> concentrations in the  
61 exhaust gas, with only CO<sub>2</sub> emissions decreasing as the ammonia share increased[16].  
62 Combining ammonia and hydrogen supply modes offers flexible fuel synergy control  
63 strategies to enhance engine performance in internal combustion engines. Rocha  
64 numerically examined premixed flame propagation and NO<sub>x</sub> emissions in  
65 ammonia/hydrogen mixed fuel, finding that while hydrogen addition accelerates flame speed,  
66 it significantly increases NO<sub>x</sub> emissions[17]. Ichikawa investigated laminar combustion rate  
67 and Markstein length in premixed combustion of ammonia-hydrogen mixtures, concluding  
68 that using hydrogen as a combustion promoter enhances power and stability, with an optimal  
69 hydrogen proportion exceeding 20%[18].  
70 In summary, most research on ammonia-hydrogen engines has concentrated on port  
71 injection, which, while convenient, reduces volumetric efficiency and power density due to  
72 H<sub>2</sub> crowding in the cylinder during the intake stroke. This inspired the present study to  
73 investigate the fuel trapping ratio at different injection timings and the velocity and turbulence  
74 fields within the cylinder under different injection timings. The research results can promote  
75 the practical application of hydrogen fuel in internal combustion engines by providing  
76 valuable insights into optimizing combustion processes and enhancing engine efficiency.  
77 This could lead to the development of more sustainable and environmentally friendly  
78 transportation solutions, contributing to the transition towards cleaner energy sources and  
79 reducing carbon emissions in the automotive sector.

## 80 81 **2. COMPUTATIONAL MODEL AND RESEARCH PROGRAM**

### 82 83 **2.1 Geometric model**

84 In this paper, a complete closed geometry model consists of inlet and exhaust port, valves  
85 and cylinder is established using the three-dimensional modeling software SolidWorks, as  
86 shown in Fig. 1(a). The basic parameters of the prototype are shown in Table 1. In order to  
87 systematically study the flow and combustion process of the mixture in-cylinder of a PFI  
88 hydrogen internal combustion engine, the initial and boundary conditions (including  
89 components, temperature, pressure, etc.) were set according to the actual working process  
90 of the internal combustion engine with the upper stopping point at the end of the  
91 compression stroke as 0 °CA. The base mesh size is 4 mm, with Adaptive Mesh Refinement

92 (AMR) implemented in high-velocity and high-temperature curvature areas. **The engine test**  
93 **bench is shown in Fig. 1 (b).**  
94



95

Formatted: Font: (Default) Arial

96

97

98 **Fig. 1. (a) 3D Engine Model (b) Engine test bench**

99

100 **Table 1. Parameters of the PFI hydrogen ICE prototype studied in this subject.**  
101

Parameters	Indexes
Connecting rod length/mm	160
Cylinder diameter/mm	94
Stroke/mm	85
Compression ratio	9.7:1
Maximum power/kW	30
Maximum power speed/r/min	6000
Maximum torque/N m	51
Maximum torque speed/r/min	4500

102

103

## 2.2 Numerical model

104

The CONVERGE software is a computational fluid dynamics software that allows the simulation of combustion, emissions, etc. The main sets of control equations are the mass conservation equation, the momentum conservation equation and the energy conservation

105

106

107 equation. In this paper, CONVERGE software is used to establish a 3D simulation model for  
 108 simulation research. The sub models used in modeling are as follows:  
 109 Turbulence model: The RNG k-ε turbulence model was chosen, which has a high accuracy  
 110 of eddy calculation and can better predict the effects of transient flows with a wider range of  
 111 applications; Spray model: CONVERGE software accurately models fuel atomization,  
 112 evaporation, crushing, and collision using the KH-RT spray fragmentation model, NTC  
 113 collision model, and wall film model for droplet-wall interaction; Combustion model: To  
 114 ensure the accuracy of the simulation study and better simulate the ignition process and  
 115 combustion process in the cylinder, the SAGE combustion model couples the n-  
 116 Heptane/hydrogen/ ammonia reaction mechanism in the simulation study.

117 **Mass conservation equation:**

$$\frac{\partial \rho}{\partial t} + \frac{\partial \rho u_i}{\partial x_i} = S \quad (1)$$

118 where:  $t$  is time; " $\rho$ " is the fluid density;  $u$  is the velocity vector; and  $S$  is the source term,  
 119 originating from evaporation or other submodels.

120 Equation of conservation of momentum:

$$\frac{\partial \rho u_i}{\partial t} + \frac{\partial \rho u_i u_j}{\partial x_j} = -\frac{\partial P}{\partial x_i} + \frac{\partial \sigma_{ij}}{\partial x_j} + S_i \quad (2)$$

$$\sigma_{ij} = \mu \left( \frac{\partial u_i}{\partial x_j} + \frac{\partial u_j}{\partial x_i} \right) + \left( \mu' - \frac{2}{3} \mu \right) \left( \frac{\partial u_k}{\partial x_k} \right) \delta_{ij} \quad (3)$$

121 where:  $t$  is time; " $\rho$ " is the fluid density;  $u$  is the velocity vector;  $S$  is the source term,  
 122 originating from evaporation or other sub-models;  $\sigma_{ij}$  is the pressure tensor;  $P$  is the  
 123 indicated pressure;  $\mu$  is the viscosity;  $\mu'$  is the expansion viscosity, which has a value of 0;  
 124 and  $\delta_{ij}$  is the Kronecker function.

125 Energy conservation equation:

$$\frac{\partial \rho e}{\partial t} + \frac{\partial u_j \rho e}{\partial x_j} = -P \frac{\partial u_j}{\partial x_j} + \sigma_{ij} \frac{\partial u_i}{\partial x_j} + \frac{\partial}{\partial x_j} \left( K \frac{\partial T}{\partial x_j} \right) + \frac{\partial}{\partial x_j} \left( \rho D \sum_m h_m \frac{\rho \gamma_m}{\partial x_j} \right) + S \quad (4)$$

126 where:  $t$  is time; " $\rho$ " is the fluid density;  $u$  is the velocity vector;  $S$  is the source term,  
 127 originating from evaporation or other sub-models;  $T$  is the temperature;  $\gamma_m$  is the mass  
 128 fraction of species  $m$ ;  $D$  is the mass diffusion coefficient;  $e$  is the specific internal energy;  
 129  $K$  is the coefficient of transport of matter; and  $h_m$  is the enthalpy of species  $m$ .

### 134 2.3 Boundary conditions and initial conditions

135 In the boundary condition settings for the PFI hydrogen-fueled internal combustion engine,  
 136 the air inlet boundary is set to the "inlet" pressure parameter type and the exhaust outlet  
 137 boundary to the "outlet" pressure parameter type. In the boundary condition setting of PFI  
 138 hydrogen fuel internal combustion engine, the air inlet boundary is set as "inlet" pressure  
 139 parameter type, and the exhaust outlet boundary is set as "outlet" pressure parameter type.  
 140 The other wall boundaries are set as "fixed wall" with constant temperature; the inlet valve,  
 141 exhaust valve and piston are set as "moving wall". Based on preliminary tests and  
 142 experience, the following boundary conditions have been established as shown in Table 2.

143 **Table 2. Boundary condition setting of PFI hydrogen engine.**

144

145

146

Border areas	Boundary type	Setpoint
Air inlet	Inlet	0.1Mpa
Exhaust outlet	Outlet	0.106Mpa
Inlet pipe	Stationary wall	300K
Exhaustpipe	Stationary wall	600K
Inlet valve	Moving wall	550K
Exhaust valve	Moving wall	800K
Cylinder wall	Stationary wall	480K
Pistons	Moving wall	600K
Cylinder head	Stationary wall	600K

147

## 2.4 Model validation

148

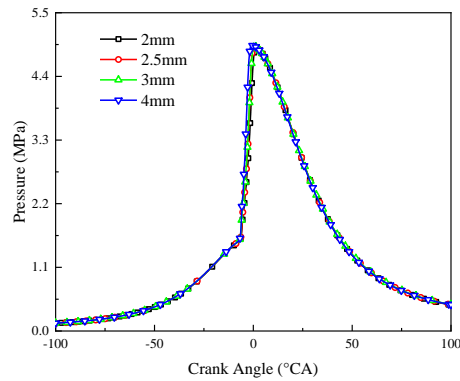
149

Fig. 2 illustrates the impact of base grid size on in-cylinder pressure, showing minor differences when the size is below 4.0 mm, thus justifying a 4 mm base grid size for simulation accuracy and efficiency.

150

151

152



153

154

**Fig.2.The effect of base grid size on in-cylinder pressure.**

155

156

157

Fig. 3 shows the comparison curves of the test and simulated in-cylinder combustion pressures of the hydrogen combustion engine under the same working conditions. It can be seen from Fig. 3 that the experimental and simulation results are in good agreement, and the maximum error is less than 5%. Therefore, it can be proved that the selected hydrogen internal combustion engine model can be used to simulate the in-cylinder combustion process, and the simulation results obtained are highly accurate.

158

159

160

161

162

163

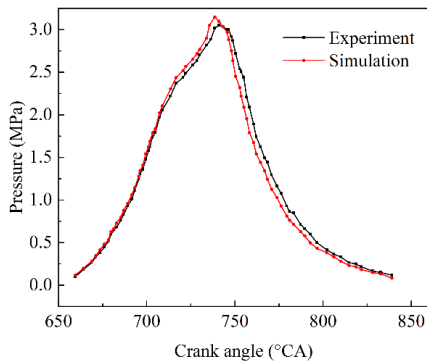


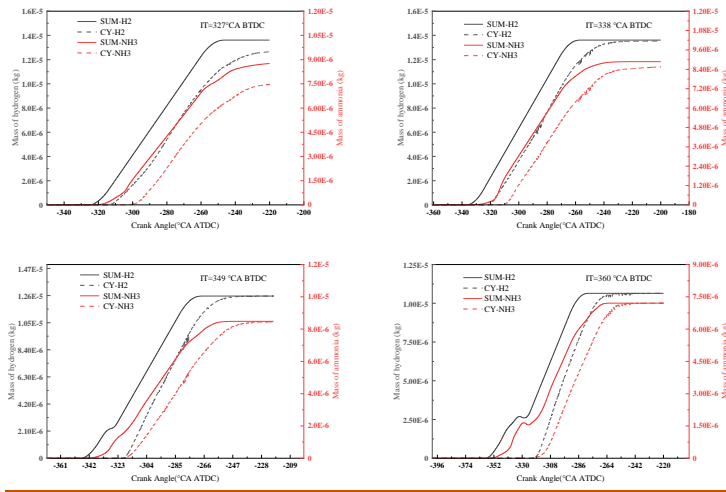
**Fig.3.In-cylinder pressure verification.**

### 2.5 Methodology

The experimental programme with different hydrogen/ammonia injection timing with four sets of hydrogen/ammonia injection timing consists of the following: H338-N338, H338-N349, H349-N338, H349-N349. Where 'H','N' denotes hydrogen/ammonia and '338','349' denotes injection timing of 338° CA BTDC and 349° CA BTDC.

An operating cycle of an internal combustion engine consists of four processes: intake, compression, work and exhaust, of which the intake process directly determines the quality of the formation of the mixed fuel and air and has an important influence on the subsequent combustion and emission processes in-cylinder. Hydrogen injection timing is an important factor in controlling the quality of hydrogen-air mixture formation, which directly influences the development and spatial-temporal distribution of hydrogen in the intake tract and into the cylinder, thus essentially inhibiting the problem of intake tract clogging in PFI hydrogen combustion engines. Selecting the optimum timing for hydrogen injection is critical to maximising performance and minimising problems such as intake tract plugging and abnormal combustion. The engine speed is 1800 rpm, the equivalence ratio is 1 and the orifice diameter is 5 mm. Fig. 4 shows the comparison between the set injection volume and the in-cylinder fuel mass at different injection timings with the intake valve closed. From the table, it is learnt that when the injection timing is 338°CA BTDC and 349°CA BTDC, the injection efficiency is the highest and the in-cylinder fuel quality meets the requirements, so the injection timing of 338°CA BTDC and 349°CA BTDC is used as the basis for the next study.

164  
165  
166  
167  
168  
169  
170  
171  
172  
173  
174  
175  
176  
177  
178  
179  
180  
181  
182  
183  
184  
185  
186  
187  
188  
189  
190

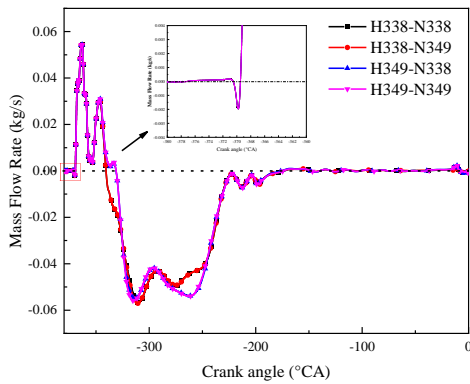


191  
192  
193 **Fig.4.In-cylinder fuel capture at different IT.**  
194

195 **3. RESULTS AND DISCUSSION**  
196

197 **3.1 Effect of injection timing on air flow in the intake pipe**

198 Figure 5 shows the variation of inlet charge mass flow rate with engine crankshaft angle  
199 corresponding to five injection timings: H338-N338, H338-N349, H349-N338, H349-N349. In  
200 Fig. 5, the vertical coordinate represents the charge inlet mass flow rate, with negative values  
201 characterising normal charge flow into the inlet and positive values characterising  
202 abnormal charge backflow out of the inlet, representing the occurrence of intake blockage.  
203 The increases and decreases described below are based on the zero tick mark, and the  
204 increases and decreases are compared in absolute magnitude.  
205  
206



207  
208 **Fig.5.Variation of air mass flow with crankshaft under different IT**  
209  
210

211 The results in Fig. 5 show that for different injection timing, when the air inlet is opened, the  
212 inlet mass flow rate increases slightly in the direction of the inflow inlet and then starts to  
213 increase in the direction of the outflow inlet and crosses the zero tick mark, increases rapidly  
214 to a peak and then returns to close to the zero tick mark, and then increases again in the  
215 direction of the outflow inlet to a peak before returning to the negative range. This is due to  
216 the initial period of intake, the valve lift is low, the charge into the intake pipe is hindered,  
217 filling the intake pipe after the intake pipe backflow phenomenon occurs, with the gradual  
218 opening of the intake valve, the backflow phenomenon is weakened. After the start of the  
219 injection timing, due to the small molecular weight of hydrogen, hydrogen is rapidly  
220 expanded after being injected into the intake tract, resulting in a rapid increase of the intake  
221 mass flow along the outflow direction of the intake tract, and air is rapidly expanded by the  
222 hydrogen and forced out of the intake tract, i.e. the air in the intake tract is a backflow  
223 phenomenon. This phenomenon is referred to as inlet air blocking phenomenon. At the end  
224 of hydrogen injection, there is no more hydrogen expansion and as the piston moves  
225 downwards, hydrogen/ammonia is pushed into the cylinder by the air and the air obstruction  
226 by hydrogen is reduced and the charge in the intake tract is always in the inflow direction  
227 and there is no intake tract backflow. When the hydrogen injection timing was earlier (338°  
228 CA BTDC), the intake tract blockage was relieved relatively early, which was more  
229 conducive to mixing fuel and air in the cylinder.

230

### 231 **3.2 Effect of Injection Timing on Velocity Field**

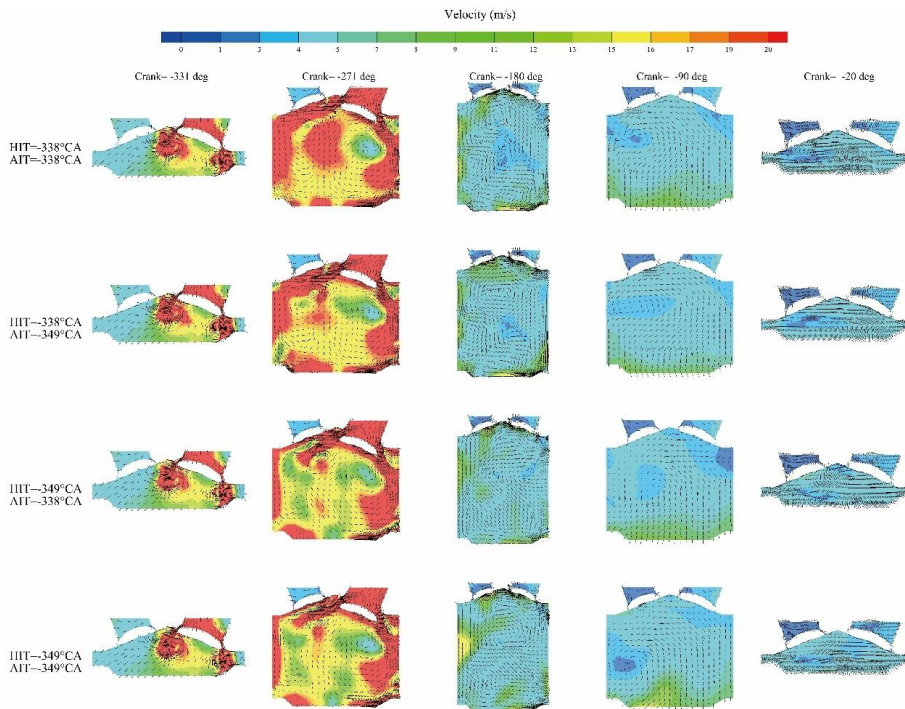
232 Varying the timing of hydrogen injection is of great importance to the law of variation of the  
233 in-cylinder velocity field in hydrogen engines. By analysing the velocity field, it is possible to  
234 gain insight into the flow characteristics of hydrogen in the combustion chamber, thus  
235 optimising the combustion process and improving engine efficiency and performance.

236 As can be seen from the figure, in-cylinder mixture at the beginning of the pressure under  
237 the action of the rapid flow to the cylinder. Following an impediment encountered at the  
238 intake valve, the amalgamated mixture navigates through a circular conduit between the  
239 intake valve and the cylinder head, ultimately coalescing into a localized region of  
240 heightened velocity proximal to the intake valve seat. At this juncture, the confined space  
241 within the cylinder constrains the voluminous influx, prompting the high-velocity mixture to  
242 collide with the cylinder head and piston crown, thereby engendering a pair of counter-  
243 rotating vortices under the influence of geometric boundaries.

244 As the intake valve opening continues to increase, the mixture fills the in-cylinder space at a  
245 higher flow rate under the effect of injection push and space expansion, and the fuel and air  
246 are further mixed. After the piston reaches the lower stop, the in-cylinder space reaches its  
247 maximum and the overall flow rate of the mixture slows down. As the compression stroke  
248 begins and the piston travels upward, the high flow velocity of the mixture gradually  
249 dissipates, with the high flow velocity area existing only at the top of the piston, and the  
250 velocity field in other areas being nearly uniformly distributed at an overall velocity. At the  
251 moment of ignition, the mixture velocity in-cylinder converges and the velocity field is  
252 uniformly distributed.

253 Longitudinal comparison shows that the velocity field of the mixture in the cylinder does not  
254 change significantly at the beginning of the intake period, and that, overall, areas of high flow  
255 velocity are formed around the valves. Before the piston moves to the lower stop, as the  
256 injection timing is delayed, the area of the high-speed area in the cylinder decreases, which  
257 is not conducive to rapid mixing of air and fuel; At the beginning of the compression stroke,  
258 the high-speed mixture in the cylinder is gradually distributed to the right side of the piston  
259 and the left side of the cylinder wall, and the whole tends to be more homogeneous; when  
260 the piston moves to the upper stop, the timing of the hydrogen/ammonia injection is all for  
261 the -330° CA conditions, with a more uniform distribution of the velocity field.

262



263

264

265

266

267

268

**Fig. 6. The development process of the velocity field**

269

### 3.3 Effect of Injection Timing on TKE

270

271

272

273

274

275

276

277

278

279

280

281

282

283

284

285

286

287

288

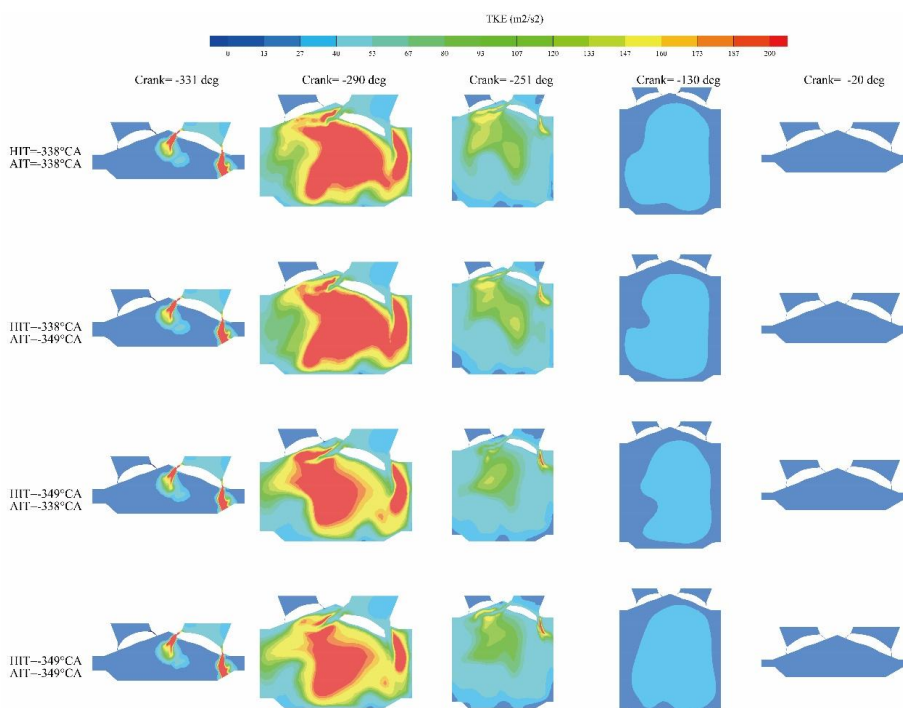
289

In practical operation, the port fuel injection (PFI) hydrogen internal combustion engine constantly undergoes a turbulent and highly disordered motion within the confines of its cylinder. Such a phenomenon exerts a discernible influence on the spatio-temporal distribution of various components and the dynamics of both the air-fuel mixture and the flame propagation, thereby exerting a formidable influence on the quality of mixture formation, combustion processes and emission characteristics.

As shown in Fig. 7, at the very beginning of the intake stroke, the high flow rate of the mixture enters the combustion chamber through the valves, and high intensity turbulence is formed around the intake valves, which corresponds to the large scale vortex clusters in the velocity field. As the piston moves down and the intake valve opens, a large amount of gas enters the cylinder along the intake valve and cylinder wall, with higher turbulent kinetic energy at the centre of the cylinder guided by the wall. Towards the end of the inlet stroke, the high turbulent kinetic energy mixture dissipates into low-intensity turbulence, thus favouring homogeneous mixing of the mixture. During the compression stroke, the turbulent kinetic energy enhanced by the compression stress and the shear force between the gas and the wall is not enough to compensate for the rapid dissipation of the turbulent vortices. At this point, the average turbulent kinetic energy in-cylinder continues to decrease. With the upward movement of the piston, the large-scale turbulent vortices continue to break up into small-scale turbulent vortices, and the turbulent motion in-cylinder gradually develops to be

290 dominated by the small-scale turbulent vortices, and the turbulent kinetic energy can be  
 291 enhanced accordingly.  
 292 A comprehensive comparison shows that the initial high turbulence kinetic energy area is  
 293 larger when the injection timing is advanced. The advance in injection timing results in the  
 294 mixture entering the cylinder earlier, which encourages a more even distribution of the  
 295 mixture in-cylinder. This advance in injection results in better mixing of the mixed fuel with  
 296 the air in-cylinder, ensuring that the fuel and oxygen are in full contact to form a more  
 297 homogeneous mixture. As a result, at the moment of ignition, the fuel can be burned more  
 298 quickly and fully, thus improving combustion efficiency and combustion performance. In  
 299 addition, injection timing advance also helps to reduce the stagnation time of the mixture in-  
 300 cylinder, reducing incomplete combustion and emissions.

301  
 302



303

304

305

306

307

308 **Fig. 7. Changes of turbulent kinetic energy in the cylinder**

309

310 **4. CONCLUSION**

311

312 By studying the spatial distribution characteristics and change laws of total hydrogen quality  
 313 inside and outside the cylinder, velocity field and turbulent kinetic energy of hydrogen  
 314 internal combustion engine under different injection timings in the intake pipe, the influence  
 315 of these parameters on the hydrogen-ammonia-air mixture formation process is revealed.  
 316 The main findings are shown below.

317

To improve the uniformity of the gas mixture, the hydrogen injection should be neither too  
 318 early nor too late. the relative residence time of the high concentration gas mixture in the

319 intake is longer if the injection is too early, which easily leads to backfire. If the hydrogen  
320 injection is late, the increase in cylinder pressure hinders the process of the hydrogen  
321 entering the cylinder. This also increases the dwell time of the hydrogen at the intake valve.  
322 At this point, the mixture will be less uniform. If the hydrogen injection is delayed, the  
323 residual hydrogen in the intake pipe can also increase, which increases the possibility of  
324 backfire. Therefore, in a comprehensive consideration, the optimum starting point for  
325 hydrogen/ammonia injection should be 338°C.

326 Future areas of research will include further optimisation of injection timing, considering  
327 sequential hydrogen/ammonia injection or multiple injection.

### 328 **ACKNOWLEDGEMENTS**

329

330 Funding: This work is supported by the Project of Educational Commission of Henan  
331 Province of China (No. 23A470012).

332

### 333 **COMPETING INTERESTS**

334

335 The authors declare that they have no known competing financial interests or personal  
336 relationships that could have appeared to influence the work reported in this paper.

337

### 338 **AUTHORS' CONTRIBUTIONS**

339

340 **Shuman Guo**: Conceptualization, Methodology, Validation, Formal analysis, Writing-original  
341 draft, Writing – review & editing. **Zhichao Lou**: Software, Investigation, Formal analysis,  
342 Writing - original draft. **Xu Zhang**: Software, Formal analysis. **Shaokai Shen**: Investigation,  
343 Software, Formal analysis. **Jintao Meng**: Data curation. **Jiaqi Wang**: Data curation. **Chunjian**  
344 **Zhou**: curation.

345

### 346 **REFERENCES**

347

- 348 1. Shang W, Yu X, Shi W, Chen Z, Liu H, Yu H, et al. An Experimental Study on  
349 Combustion and Cycle-by-Cycle Variations of an N-Butanol Engine with Hydrogen Direct  
350 Injection under Lean Burn Conditions. *Sensors* 2022;22:1229.  
351 <https://doi.org/10.3390/s22031229>.
- 352 2. Ishii T, Yamada K, Osuga N, Imashiro Y, Ozaki J. Single-Step Synthesis of W2C  
353 Nanoparticle-Dispersed Carbon Electrocatalysts for Hydrogen Evolution Reactions  
354 Utilizing Phosphate Groups on Carbon Edge Sites. *ACS Omega* 2016;1:689–95.  
355 <https://doi.org/10.1021/acsomega.6b00179>.
- 356 3. Thermo - environomic evaluation of the ammonia production - Tock - 2015 - The  
357 Canadian Journal of Chemical Engineering - Wiley Online Library n.d.  
358 <https://onlinelibrary.wiley.com/doi/abs/10.1002/cjce.22126> (accessed March 14, 2024).
- 359 4. Gao J, Zhang H, Li J, Wang Y, Tian G, Ma C, et al. Simulation on the effect of  
360 compression ratios on the performance of a hydrogen fueled opposed rotary piston  
361 engine. *Renew Energy* 2022;187:428–39. <https://doi.org/10.1016/j.renene.2022.01.091>.
- 362 5. Nag S, Dhar A, Gupta A. Hydrogen-diesel co-combustion characteristics, vibro-acoustics  
363 and unregulated emissions in EGR assisted dual fuel engine. *Fuel* 2022;307:121925.  
364 <https://doi.org/10.1016/j.fuel.2021.121925>.
- 365 6. Benbellil MA, Lounici MS, Loubar K, Tazerout M. Investigation of natural gas enrichment  
366 with high hydrogen participation in dual fuel diesel engine. *Energy* 2022;243:122746.  
367 <https://doi.org/10.1016/j.energy.2021.122746>.
- 368 7. Xin G, Ji C, Wang S, Meng H, Chang K, Yang J. Effect of different volume fractions of  
369 ammonia on the combustion and emission characteristics of the hydrogen-fueled

- 370 engine. Int J Hydrog Energy 2022;47:16297–308.  
371 <https://doi.org/10.1016/j.ijhydene.2022.03.103>.
- 372 8. Frigo S, Gentili R. Analysis of the behaviour of a 4-stroke Si engine fuelled with ammoni  
373 a and hydrogen. Int J Hydrog Energy 2013;38:1607–15. <https://doi.org/10.1016/j.ijhydene.2012.10.114>.
- 374
- 375 9. Wang B, Yang C, Wang H, Hu D, Wang Y. Effect of Diesel-Ignited Ammonia/Hydrogen  
376 mixture fuel combustion on engine combustion and emission performance. Fuel  
377 2023;331:125865. <https://doi.org/10.1016/j.fuel.2022.125865>.
- 378 10. Zhang R, Chen L, Wei H, Li J, Chen R, Pan J. Understanding the difference in  
379 combustion and flame propagation characteristics between ammonia and methane  
380 using an optical SI engine. Fuel 2022;324:124794.  
381 <https://doi.org/10.1016/j.fuel.2022.124794>.
- 382 11. Dimitriou P, Javaid R. A review of ammonia as a compression ignition engine fuel. Int J  
383 Hydrog Energy 2020;45:7098–118. <https://doi.org/10.1016/j.ijhydene.2019.12.209>.
- 384 12. Chen J, Jiang X, Qin X, Huang Z. Effect of hydrogen blending on the high temperature  
385 auto-ignition of ammonia at elevated pressure. Fuel 2021;287:119563.  
386 <https://doi.org/10.1016/j.fuel.2020.119563>.
- 387 13. Zhu X, Khateeb AA, Guiberti TF, Roberts WL. NO and OH\* emission characteristics of  
388 very-lean to stoichiometric ammonia–hydrogen–air swirl flames. Proc Combust Inst  
389 2021;38:5155–62. <https://doi.org/10.1016/j.proci.2020.06.275>.
- 390 14. Oh S, Park C, Kim S, Kim Y, Choi Y, Kim C. Natural gas–ammonia dual-fuel combustion  
391 in spark-ignited engine with various air–fuel ratios and split ratios of ammonia under part  
392 load condition. Fuel 2021;290:120095. <https://doi.org/10.1016/j.fuel.2020.120095>.
- 393 15. Grannell SM, Assanis DN, Gillespie DE, Bohac SV. Exhaust Emissions From a  
394 Stoichiometric, Ammonia and Gasoline Dual Fueled Spark Ignition Engine, American  
395 Society of Mechanical Engineers Digital Collection; 2009, p. 135–41.  
396 <https://doi.org/10.1115/ICES2009-76131>.
- 397 16. Şahin Z, Ziya Akcanca İ, Durgun O. Experimental investigation of the effects of ammonia  
398 solution (NH<sub>3</sub>OH) on engine performance and exhaust emissions of a small diesel  
399 engine. Fuel 2018;214:330–41. <https://doi.org/10.1016/j.fuel.2017.10.034>.
- 400 17. da Rocha RC, Costa M, Bai X-S. Chemical kinetic modelling of ammonia/hydrogen/air  
401 ignition, premixed flame propagation and NO emission. Fuel 2019;246:24–33.  
402 <https://doi.org/10.1016/j.fuel.2019.02.102>.
- 403 18. Ichikawa A, Hayakawa A, Kitagawa Y, Kunkuma Amila Somarathne KD, Kudo T,  
404 Kobayashi H. Laminar burning velocity and Markstein length of ammonia/hydrogen/air  
405 premixed flames at elevated pressures. Int J Hydrog Energy 2015;40:9570–8.  
406 <https://doi.org/10.1016/j.ijhydene.2015.04.024>.
- 407 19. Tan D, Meng Y, Tian J, Zhang C, Zhang Z, Yang G, et al. Utilization of renewable and  
408 sustainable diesel/methanol/n-butanol (DMB) blends for reducing the engine emissions  
409 in a diesel engine with different pre-injection strategies. Energy 2023;269:126785.  
410 <https://doi.org/10.1016/j.energy.2023.126785>.
- 411